Received January 14, 2021, accepted January 28, 2021, date of publication February 23, 2021, date of current version March 15, 2021.

Digital Object Identifier 10.1109/ACCESS.2021.3058243

Research on Temperature and Braking Performance of Water-Cooled Eddy Current Retarder

XIANGLI LI, LEZHI YE, MINGFEI LI, AND QIANG LV

Faculty of Material Manufacturing, Beijing University of Technology, Beijing 100124, China

Corresponding author: Lezhi Ye (yelezhi@bjut.edu.cn)

This work was supported in part by the Science and Technology Program of Beijing Municipal Education Commission under Grant KM 201710005010, and in part by the National Natural Science Foundation of China under Grant 51741701.

ABSTRACT Trucks have the problems of frequent braking and long-term braking during long-slope transportation. As the temperature of the traditional eddy current retarder is as high as 500 °C during braking, the braking torque of the retarder is seriously degraded. According to the principle of eddy current braking and current thermal effect, this paper proposes an eddy current retarder in which both the stator and the excitation coil are water-cooled. The multi-field coupling and bidirectional data transmission model of stator temperature field, coil temperature field and transient electromagnetic field are established. The relationship between the braking torque and the working time is analyzed under continuous braking conditions, considering the stator temperature and the temperature of the excitation coil. It provides theoretical support for the optimal design of the retarder. A test prototype of a water-cooled eddy current retarder was manufactured, and a bench drag test was carried out. The calculation results show that the numerical simulation method of coupling between the stator temperature field, the coil temperature field and the transient electromagnetic field is adopted, and the simulation values of the braking torque is in good agreement with the experimental values.

INDEX TERMS Braking torque, excitation coil, eddy current retarder, multi-field coupling, water cooling.

I. INTRODUCTION

As a non-contact auxiliary braking device, the eddy current retarder can convert the mechanical energy of the vehicle into thermal energy by the principle of eddy current braking to achieve vehicle braking [1], [2]. The eddy current retarder generates lots of heat when continuous braking, which makes the braking torque degrade seriously and reduces reliability.

Aiming at the problem of thermal degrade of the braking torque of the eddy current retarder, domestic and foreign scholars have studied the electromagnetic field, temperature field, structural optimization and braking characteristic test of the eddy current brake devices [3]–[7]. Professor Feng Yaojing of Hunan University proposed an oil cooling system, combined with the method of fluid simulation to analyze the rotor temperature distribution of the high-power eddy current retarder [8]. Tais *et al.* proposed an optimization method combining finite element and sensitivity analysis to optimize the rotor structure [9]. Liu Yupeng *et al.* proposed a flywheel eddy current retarder with water cooling method, which used computational fluid dynamics method to analyze the hydrothermal coupling field [10]. Jin Y *et al.* used the electromagnetic field model and the magnetic-thermal coupling model to calculate the temperature distribution and braking torque of the Halbach retarder [11]. They studied the structure and temperature field of the retarder, improved the cooling method of the retarder and considered the influence of temperature on the permeability and conductivity of the material [12]–[15]. However, the influence of the thermal effect of the excitation current on the braking torque under the continuous braking condition of the retarder is ignored, and the resistance of the excitation coil increases and the current decreases due to the high temperature.

This paper proposes a new type of water-cooled eddy current retarder, whose stator and electromagnetic coil are designed as a water-cooled structure. A coupling model to explore the impact of temperature on braking torque is established. The relationship between braking torque and working

The associate editor coordinating the review of this manuscript and approving it for publication was Xiaokang Yin.

time is obtained. The braking performance of the retarder is improved under continuous braking condition.

II. STRUCTURE AND WORKING PRINCIPLES

In order to improve the braking performance of the water-cooled eddy current retarder, a new eddy current retarder in which the stator and excitation coil are both designed as water-cooled is proposed. The structure of the new water-cooled eddy current retarder is shown in Fig 1. It is mainly composed of a stator, a rotor, a coil, a rotor connection, a water inlet and a water outlet. The stator of the retarder is provided with inner and outer water channels, and the inner and outer water channels are connected with the coil water channel. When the retarder is working, the excitation coil forms a closed circular magnetic field on the stator and rotor. The rotation of the salient poles inside and outside the rotor changes the magnetic field. Eddy currents are generated on the surface of the stator. The intensity of the eddy currents is controlled by the coil current. The eddy currents will excite the magnetic field to suppress the changes in the original annular magnetic field and generate braking torque.

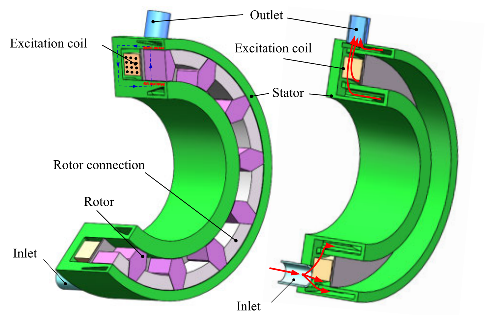

FIGURE 1. The structure of new water-cooled eddy current retarder.

When the new water-cooled eddy current retarder is cooled, the coolant flows into the retarder through the water inlet, and flows in three ways according to the principle of the communicating vessel: the inner water channel, the outer water channel and the coil water channel, so that the temperature of the retarder stator and the excitation coil is cooled. It solves the problems of braking torque decay caused by high temperature under continuous braking conditions, such as the decrease of stator permeability and conductivity, and the instability of excitation coil current.

III. ELECTROMAGNETIC FIELD ANALYSIS

A. MAGNETIC EQUIVALENT CIRCUIT METHOD

When the new water-cooled eddy current retarder is designed, the magnetic circuit method is used to calculate the static air gap magnetic field [16], [17]. Fig 2 shows the equivalent magnetic circuit model of the retarder. Fig 2(a) is a simplified three-dimensional model of the retarder. Since the rotor connection is made of non-magnetic material, it can be ignored in modeling. The structural parameters of the retarder are shown in Table 1.

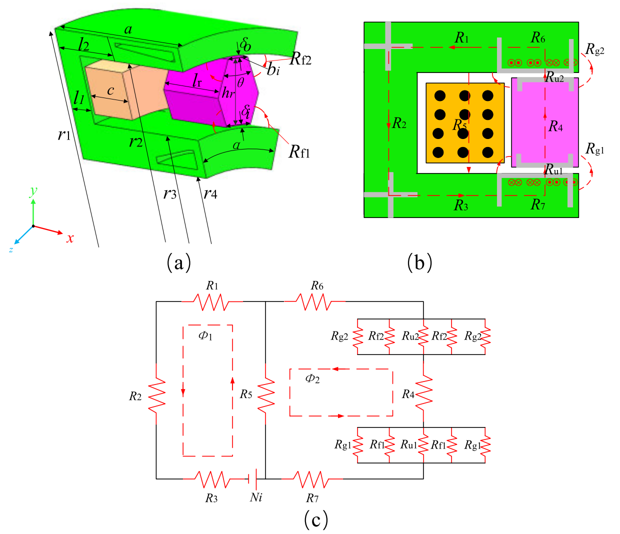

FIGURE 2. The equivalent magnetic circuit model of retarder. a) Three-dimensional simplified model. b) Cross section. c) Equivalent magnetic circuit model.

TABLE 1. Design parameters of retarder.

	Sign	Parameter	Unit	Value
Stator	r_1	Outer radius	mm	225
	r_2	Outside working radius	mm	206
	r_3	Inner working radius	mm	152
	r_4	Inner radius	mm	122
	a	Length	mm	138
Rotor	l_r	Tooth length	mm	56
	b_1	Width of external teeth	mm	19
	b_2	Width of internal teeth	mm	23
	h_r	Tooth height	mm	52.4
Air gap	δ_o	External working air gap	mm	0.8
	δ_i	Inner working air gap	mm	1
	α	Cycle angle	deg	30

Fig 2(b) ignores the influence of the water channel, $R_1, R_2, R_3, R_4, R_6, R_7$ are the magnetic resistance of soft magnetic materials, R_{u1}, R_{u2} are the air gap magnetic resistance, they can be calculated by (1).

$$R = \frac{l}{\mu (B, T) \cdot s} \tag{1}$$

where l is the equivalent length of the magnetic resistance, s is the equivalent cross-sectional area of the magnetic resistance, the magnetic permeability μ is a function of the magnetic induction intensity B and the temperature T.

$$\frac{1}{\mu (B,T)} = \frac{-\mu_0 h - M + B + \sqrt{(\mu_0 h + M - B)^2 + 4\mu_0 hB}}{2k(T)B\mu_0} \tag{2}$$

where $h = 1000$, $M = 2$ is the constant for the 20# steel, and $k(T)$ is the temperature coefficient.

R_{f1}, R_{f2}, R_{g1}, R_{g2} are edge leakage magnetic resistance, they can be calculated by (3) and (4).

$$F = Ni(T) = \int H \cdot dl \tag{3}$$

$$R = \frac{F}{\mu_0 sH} \tag{4}$$

where F is the magnetic potential, N is the number of turns of the coil, i is a function of the temperature T, and H is the magnetic field strength.

R_5 is the leakage magnetic resistance of the slot can be calculated by formula (5).

$$R_5 = \frac{1}{\frac{2\alpha\mu_0 r_3[3(a-l_1-l_r)-2c]}{3(r_2-r_3)}} \tag{5}$$

The static air gap flux density B_0 is obtained by the mesh analysis formulation algorithm, as in formula (6)

$$R_N \cdot \phi_N = F_N \tag{6}$$

where Φ is the magnetic flux.

B. TRANSIENT MAGNETIC FIELD

When the new water-cooled eddy current retarder continues to work, the magnetic permeability and electrical conductivity of the stator material and the current of the excitation coil are affected by temperature. To improve the reliability of the magnetic field analysis, it is necessary to perform finite element analysis on the transient magnetic field of the retarder. The skin effect makes the eddy current concentrate on the surface of the stator, and the skin depth can be expressed as:

$$\Delta = \sqrt{\frac{2}{\omega\mu\sigma}} \tag{7}$$

where ω is the angular velocity of the rotor, μ is the magnetic permeability, σ is the electrical conductivity.

To obtain more accurate simulation results, the skin depth is divided into 3 layers, and the mesh division result is shown in Fig 3. The number of meshes obtained is 116498 and the number of nodes is 44852.

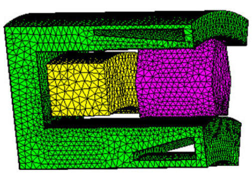

FIGURE 3. Mesh division.

When the new water-cooled eddy current retarder speed is 1000r/min and the current of the excitation coil is 80A, the transient magnetic field is analyzed. Fig 4 (a) is the distribution diagram of the transient magnetic field of the retarder. From the figure, the structure of the retarder is reasonable and the magnetic density distribution of each part is close to saturation. Fig 4(b) shows the eddy current density distribution trend on the inner wall of the stator. Due to the armature reaction, the eddy current density on the side of the rotor teeth is greater.

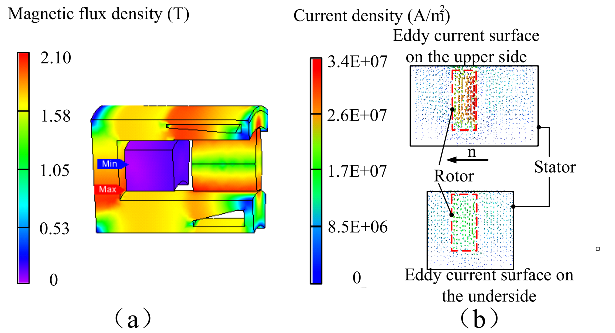

FIGURE 4. Transient magnetic field analysis. a) Magnetic field distribution diagram. b) Eddy current distribution diagram.

IV. COUPLED FIELD ANALYSIS

A. COUPLED FIELD NUMERICAL MODEL

The new water-cooled eddy current retarder generates a lot of heat under continuous braking conditions, which will affect the electromagnetic characteristics of the retarder itself. To obtain an accurate braking characteristic curve, this paper uses the multi-field coupling method to establish a numerical model. Including physical fields such as electromagnetic field, temperature field and fluid field, Table 2 shows the thermophysical properties of each part. The finite element method is used for coupling calculation of the physical field, and the calculation process is shown in the Fig 5.

TABLE 2. Thermophysical properties of parts.

Part	Material	Thermal Conductivity (W/m•k)	Density (kg/m³)	Specific Heat Capacity (J/kg•K)
Stator	20 steel	49	7850	512
Insulatec wire	Teflon	0.24	2100	1050
Coolant	Water	0.604	997.4	4179
Coil	Copper	400	8933	385

Firstly, the finite element model of the retarder's transient electromagnetic field, stator temperature field and coil temperature field are established. The initial conditions of the finite element model and calculate the electromagnetic field are set. The stator temperature field of the retarder is calculated by the eddy current loss power as the heat source. The heat of stator can change the parameters of the transient electromagnetic field, and the electromagnetic parameters of the stator material in the electromagnetic field are corrected according to the updated temperature. The coil Joule loss power is taken as the heat source to calculate the coil temperature field. The coil temperature corrects the excitation current of the coil in the electromagnetic field. At this time, the electromagnetic field starts a new calculation. After multiple iterations, the calculation stops when the working time is 12 minutes.

In the transient electromagnetic field calculation, the braking torque of the retarder is calculated according to the initial conditions, and the relationship between μ and σ of the

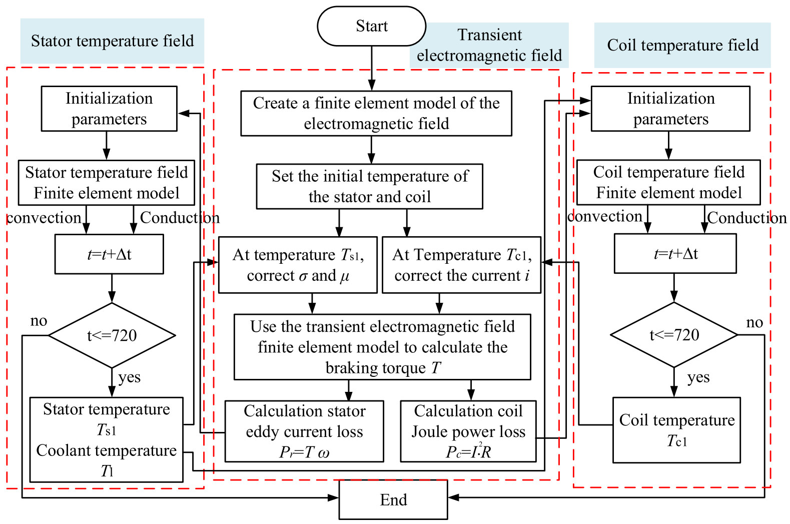

FIGURE 5. Coupling calculation flow chart.

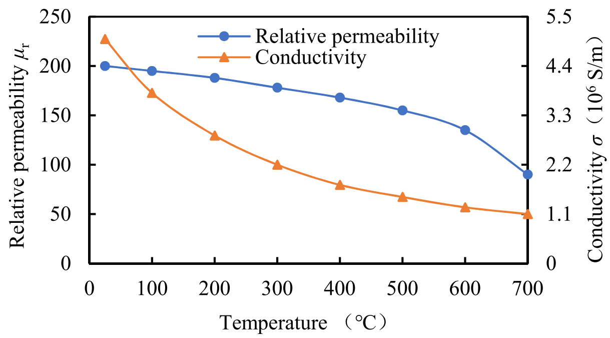

FIGURE 6. The relationship between electrical conductivity and magnetic permeability with temperature.

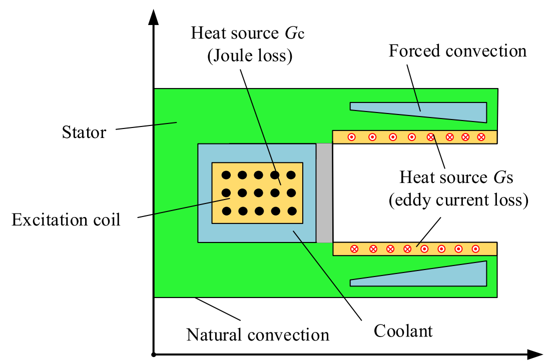

FIGURE 8. Temperature field calculation model.

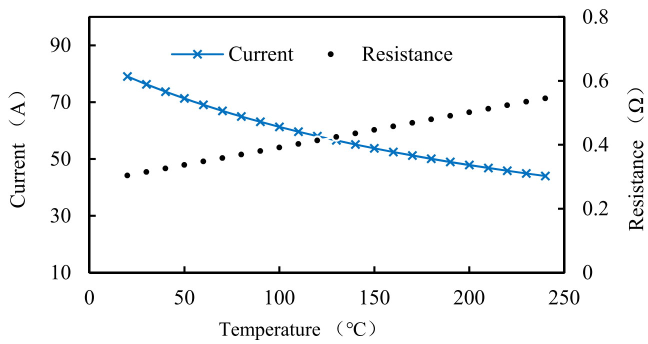

FIGURE 7. Resistance characteristics change with temperature.

stator material and temperature, and the relationship between the resistance characteristics of the coil and temperature are considered in the iteration process, as shown in Fig 6 and Fig 7.

B. STATOR TEMPERATURE FIELD MODEL OF RETARDER

The heat source of new water-cooled eddy current retarder is mainly divided into two parts, one part is the Joule loss caused by the direct current applied to the excitation coil, and the other part is the eddy current loss caused by the eddy current on the stator surface. In order to study the effect of stator temperature change on braking torque under continuous braking conditions, a calculation model of retarder stator temperature field was established, as shown in Fig 8. In the calculation process, the following assumptions were made: (1) The coolant is a constant substance and flows in one direction; (2) The stator material is an isotropic thermal conductivity medium; (3) The main heat generating part of the stator material passes through the coolant to cool down by forced convection, ignoring the heat transferred by radiation.

When the new water-cooled eddy current retarder works, eddy current loss is generated on the stator working surface corresponding to the rotor teeth, and the eddy current loss power is used as the heat source, and its heating power is approximately equal to the braking power. As shown in Fig 9, the braking torque generated by the upper and lower eddy current surfaces is obtained by the multi-field coupling method. Under the influence of temperature, the upper eddy current surface thermally degrades by 12.9%, and the lower vortex surface thermally degrades by about 20.2%. The heat generation rate is calculated as:

$$G_S = \frac{P_E}{V_E} = \frac{T_E \omega}{V_E} \tag{8}$$

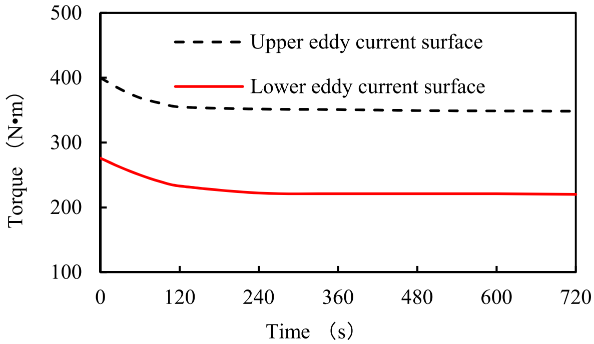

FIGURE 9. Braking torque of upper and lower eddy current surfaces.

where G_S is the heat generation rate, P_E is the eddy current loss power, V_E is the equivalent volume of the eddy current loss part, and T_E is the retarder braking torque.

The mass flow rate at the inlet of the fluid domain is 1 kg/s, the temperature is 25°, and the outlet pressure is atmospheric pressure. Under these conditions, working continuously for 12 minutes, the retarder temperature distribution diagram is shown in Fig 10(a). The maximum temperature is 360°, and the high temperature area mainly concentrates on the eddy current loss area on the inner surface of the stator. Fig 10(b) shows the temperature distribution of the retarder channel, and the highest temperature is 140.5°. Since the coolant has a cooling effect on the retarder, the high-temperature area distribution of the coolant corresponds to the high-temperature area of the stator.

the stator.

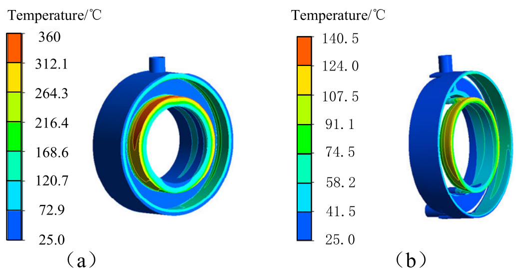

FIGURE 10. Temperature distribution diagram of retarder. a) Overall temperature. b) Waterway temperature.

As shown in Fig 11, when the retarder continues to work for 12 minutes, the average temperature of the upper and lower eddy current surfaces changes with time. Within 0-0.6 minutes, because the heat generated by the outer working surface is taken away by the coolant in time, the temperature of this part is stabilized firstly. Within 0.6-2.8 minutes, the temperature of the inner working surface is higher than that of the outer working surface, and gradually tends to be stable, because the inner working surface is farther from the water channel than the outer working surface, and the cooling time of the cooling liquid on the inner working surface is longer than that of the outer working surface. On the other

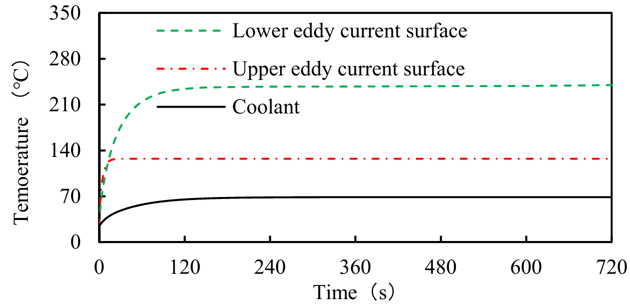

FIGURE 11. Temperature curve of the retarder continuously working.

hand, the average temperature of the cooling liquid has gradually stabilized from 25° to 68°.

C. TEMPERATURE FIELD MODEL OF COIL

When analyzing the stator temperature field of the new water-cooled eddy current retarder, the coil is simplified into a ring part. This method can only simulate the temperature change of the retarder stator, but cannot simulate the temperature change inside the coil, and cannot accurately analyze the effect of temperature on the excitation current. Therefore, this paper establishes the coil temperature field calculation model, as shown in Fig 12. Using the Joule power generated by the coil as the heat source, heat is transferred between the insulated wire, copper and the cooling liquid through heat conduction, and the coil is cooled by the cooling liquid through forced convection.

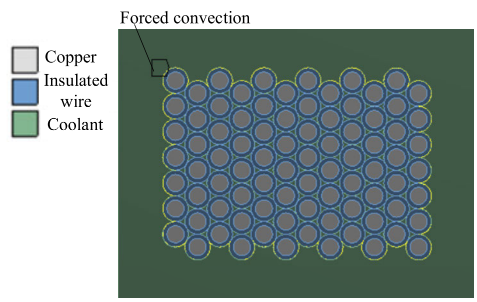

FIGURE 12. Coil temperature field calculation model.

The heat generated by Joule loss is applied to the copper of the excitation coil, and the average temperature of the coolant in the retarder stator temperature field is transferred to the coolant temperature in the coil temperature field. As shown in the Fig 13, the coil Joule loss power and coolant temperature, the heat generation rate of the coil:

$$G_C = \frac{U^2}{R_C V_C} = \frac{P_C}{V_C} \tag{9}$$

where U is the coil voltage, R_C is the coil resistance, V_C is the coil equivalent volume, and P_C is the coil Joule power loss.

The temperature distribution of the coil under water-cooling conditions is shown in Fig 14(a). It can be seen from the figure that the temperature from the periphery of

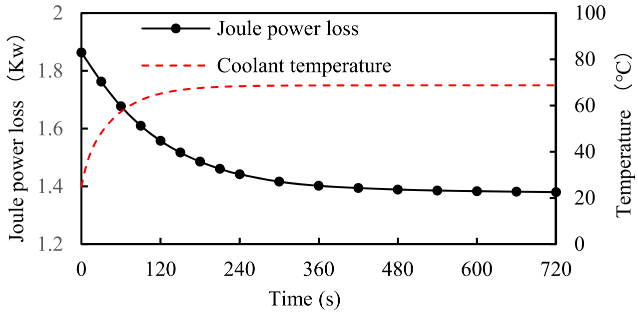

FIGURE 13. Coil Joule power loss and coolant temperature.

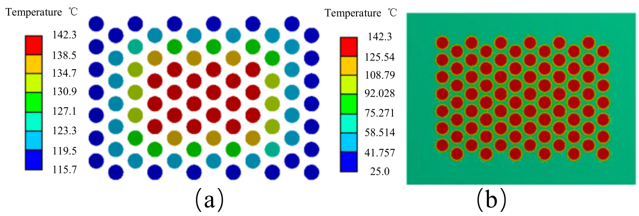

FIGURE 14. Coil temperature change curve. a) Coil copper temperature change. b) Coil temperature distribution.

the coil to the inside of the coil gradually rises. The highest temperature of the coil is 142.3° and the lowest temperature is 115.7°. Due to the difference in the contact area and convection coefficient between the wire and the coolant, the highest temperature appears inside the coil. Fig 14(b) shows the overall temperature distribution of the coil temperature field model.

When the new water-cooled eddy current retarder is working, the temperature of the excitation coil gradually increases. Under the action of forced convection and heat conduction by the coolant, the temperature of the coil tends to stabilize, and the resistance value increases with the increase in temperature. Under certain voltage conditions, the excitation current will decrease, which will affect the braking performance of the retarder. Therefore, the calculation of the coil temperature field is particularly important. Fig 15 shows the average temperature change curve of the coil. According to the coil temperature change curve in Fig. 7 and the average temperature characteristic curve of the coil in Fig. 15, the change curve of the resistance and current of the coil under water cooling conditions with the braking time during continuous braking is obtained, as shown in Fig 16. Under water-cooled conditions, the current decreases by about 24% as the braking time increases.

V. RETARDER TEST PLATFORM

The new water-cooled eddy current retarder test platform is mainly composed of drag motor, eddy current retarder, torque speed sensor, temperature sensor (including thermocouple type and infrared non-contact type), battery and Tesla meter etc. For different experimental requirements, the test platform

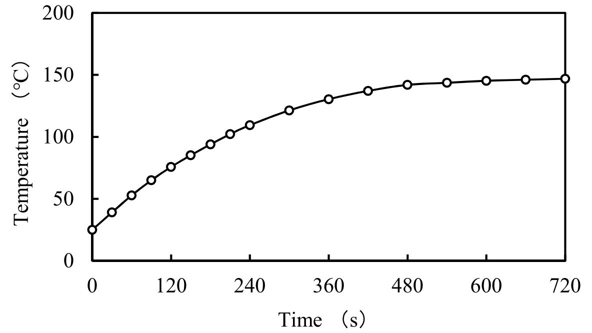

FIGURE 15. Average temperature change curve of the coil.

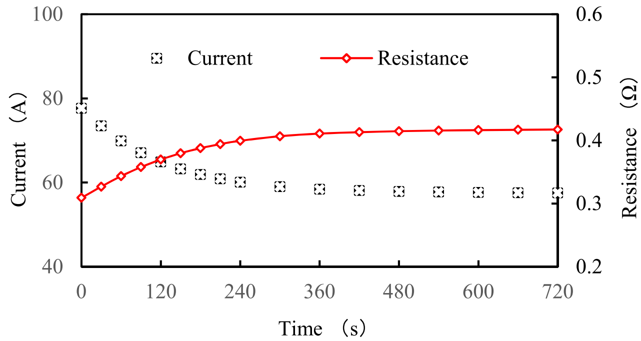

FIGURE 16. Variation curve of excitation current.

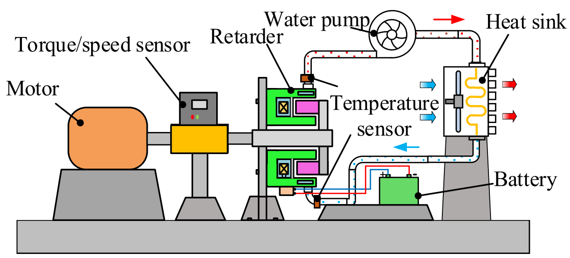

FIGURE 17. The new water-cooled eddy current retarder bench test platform.

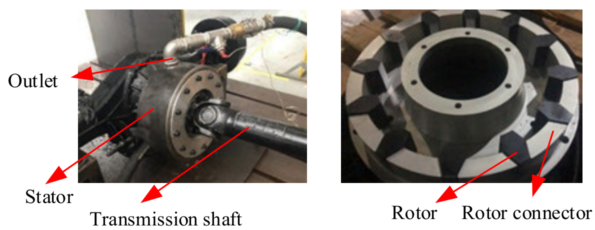

FIGURE 18. Retarder prototype.

is shown in Fig 17. To analyze the braking torque characteristics, continuous braking characteristics, and continuous braking temperature rise characteristics of the retarder, a prototype of an eddy current retarder with a water-cooled stator and coil was manufactured. And use existing instruments to collect the speed, braking torque, temperature and magnetic flux density of the prototype when it is running. The retarder prototype is shown in Fig 18.

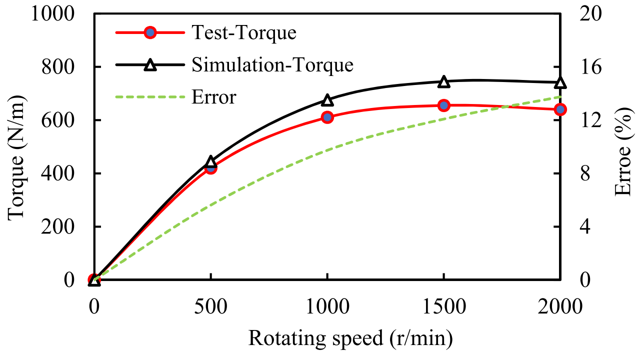

FIGURE 19. Braking torque at different speeds.

VI. RETARDER TEST PLATFORM

A. BRAKING TORQUE CHARACTERISTIC TEST

To verify the braking performance of the retarder, the retarder braking torque was tested. Under a certain current excitation, for the speed-braking torque test, the simulation and test values of the braking torque at different speeds are shown in Fig 19, and the test value of the retarder torque is in good agreement with the simulation calculation value. At 1000 r/min, the test process generates heat, which leads to changes in the permeability and conductivity of the retarder material. However, the temperature effect is not considered in the finite element analysis process, so the simulated value is greater than the experimental value, the error is 9.7%, and the error is gradually increasing.

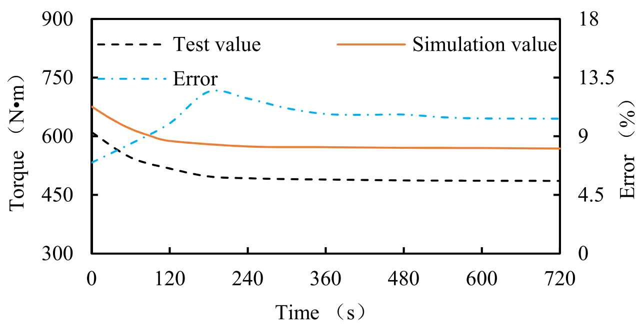

FIGURE 20. Continuous braking characteristics.

B. CONTINUOUS BRAKING CHARACTERISTIC TEST

To study the change characteristics of the braking torque of the new water-cooled eddy current retarder under continuous braking operation. When working continuously for 12 minutes at 1000r/min speed, the retarder braking torque change curve is shown in Fig 20. It can be seen from the figure that when the multi-field coupling analysis method is used, the torque simulation value of the water-cooled eddy current retarder is within 12.4% of the experimental value. As the working time increases, the temperature affects the electromagnetic properties of the material and the excitation coil current. The error between the simulated value and the experimental value first increases and then gradually decreases. The reason for the error is partly due to the coil model used in the simulation, its wire winding method is regular, the coil winding is relatively compact in the experiment, and the heat transfer of the coil is different. Another part is due to casting defects and thermal deformation of the assembled rotor.

Under the condition of continuous braking, the temperature of the retarder increases, the electromagnetic characteristics of the stator and the excitation characteristics of the coil will change, the braking torque will decrease, and it will stabilize after a period. The thermal decay rate is an index to evaluate the continuous braking ability of the retarder. The thermal decay rate is:

$$F_{hf} = \frac{(T_{\max} - T_s)}{T_{\max}} \times 100\% \tag{10}$$

where F_{hf} is the thermal decay rate, $T_{\max}$ is the transient braking torque, T_{s} is the braking torque at the end of continuous braking.

As shown in Table 3, under the water-cooled retarder structure, the thermal decay rate of braking torque in the retarder test is 20.3%, and the simulated thermal decay rate of torque is 15.9%.

TABLE 3. Torque decline under continuous braking.

	Water cooling-experiment	Water cooling-simulation
$T_{\max}$ (N·m)	610	676
T_s (N·m)	486	568.5
F_{hf} (%)	20.3	15.9

TABLE 4. Temperature before and after braking.

Test location	The initial temperature /°C	Temperature after braking /°C
Coolant	25	75
Stator housing	25	65

C. CONTINUOUS BRAKING TEMPERATURE RISE CHARACTERISTIC TEST

When the retarder continues to work, the mechanical energy of the vehicle is converted into thermal energy. The electromagnetic characteristics of the stator material and the resistance characteristics of the coil are affected by temperature, which is the main cause of the retarder's braking torque decline. The new water-cooled eddy current retarder adopts a fully water-cooled concentrated winding structure. The heat-generating retarder stator and electromagnetic coil are designed as water-cooled structures, which effectively reduces the thermal decay rate of the retarder's braking torque. During the continuous braking test, the coolant flow rate at the water inlet of the retarder is 1 kg/s, and the initial temperature is 25°. As shown in Table 4, after the test, the coolant temperature rises by 50°, and the temperature of the stator housing remains within 65°, which meets the enterprise's temperature requirements for retarders.

VII. CONCLUSION

The braking torque of the retarder is affected by temperature, which is mainly reflected in the electromagnetic characteristics of the material and the resistance characteristics of the excitation coil with temperature. During continuous operation, the temperature of the retarder's stator and excitation coil rises, and the electromagnetic characteristics and resistance characteristics tend to decrease the braking torque. The purpose of the new water-cooled eddy current retarder is to cool the stator and the excitation coil, and can take away the heat generated by the retarder in time.

The retarder's stator temperature field, coil temperature field and transient electromagnetic field coupling method are used to analyze the retarder performance during continuous braking. According to the simulation and test results, the error is gradually increased from 9.7% to 12.4% due to temperature, but as the temperature of the new water-cooled eddy current retarder stator and excitation coil stabilizes, the error gradually decreases.

The newly developed water-cooled eddy current retarder prototype has a thermal decay rate of 20.3% for the braking torque test value. The thermal decay rate of the simulation value of the braking torque analyzed by the magnetic-thermal coupling method is 15.9%. The main reason for the error is the casting defect and the thermal deformation of the assembled rotor.

REFERENCES

[1] Z. Wang, G. Tan, X. Shen, Y. Ye, Q. Zhou, and X. He, "Performance analysis of a contactless combined auxiliary brake for hybrid electric vehicle," in *Proc. IEEE Int. Transp. Electrific. Conf. (ITEC)*, Chennai, India, Aug. 2015, pp. 1–6.

[2] S. Sharif, J. Faiz, and K. Sharif, "Performance analysis of a cylindrical eddy current brake," *IET Electr. Power Appl.*, vol. 6, no. 9, pp. 661–668, Nov. 2012.

[3] Y. Jin, L. Li, B. Kou, and D. Pan, "Thermal analysis of a hybrid excitation linear eddy current brake," *IEEE Trans. Ind. Electron.*, vol. 66, no. 4, pp. 2987–2997, Apr. 2019.

[4] H. Zheng, Y. Lei, and P. Song, "Hydraulic retarders for heavy vehicles: Analysis of fluid mechanics and computational fluid dynamics on braking torque and temperature rise," *Int. J. Automot. Technol.*, vol. 18, no. 3, pp. 387–396, Jun. 2017.

[5] Y. Lezhi, L. Chen, L. Yupeng, L. Desheng, and L. Zenggang, "Performance analysis and test of a novel eddy-current braking & heating system for electric bus," *Energy Convers. Manage.*, vol. 183, pp. 440–449, Mar. 2019, doi: 10.1016/j.enconman.2019.01.010.

[6] B. Jiao, D. Li, X. Du, and K. Zhang, "Performance analysis and experimentation of a liquid-cooled eddy current retarder with a dual salient poles design," *IEEE Trans. Energy Convers.*, vol. 29, no. 1, pp. 84–90, Mar. 2014.

[7] C. Y. Liu, K. J. Jiang, and Y. Zhang, "Design and use of an eddy current retarder in an automobile," *Int. J. Automot. Technol.*, vol. 12, no. 4, pp. 611–616, Jul. 2011.

[8] F. Yaojing, X. Xiangshuai, and H. Shoudao, "Design research of high power oil-cooled electrical eddy current retarder for heavy vehicles," in *Proc. Int. Conf. Elect. Mach. Syst. (ICEMS)*, Chiba, Japan, 2017, pp. 1–5.

[9] K. V. Tatis, A. G. Kladas, and J. A. Tegopoulos, "Geometry optimization of solid rotor eddy current brake by using sensitivity analysis and 3D finite elements," *J. Mater. Process. Technol.*, vol. 161, nos. 1–2, pp. 363–367, Apr. 2005.

[10] L. Ye, Y. Liu, and D. Li, "Performance analysis and optimization of liquid-cooled and flywheel-type eddy current retarder," *IEEE Trans. Magn.*, vol. 55, no. 6, pp. 1–5, Jun. 2019.

[11] Y. Jin, B. Kou, L. Zhang, H. Zhang, and H. Zhang, "Magnetic and thermal analysis of a Halbach permanent magnet eddy current brake," in *Proc. Int. Conf. Electr. Mach. Syst.*, Chiba, Japan, 2016, pp. 1884–2021.

[12] Y. Ji, J. Wang, Y. Xu, and Z. Li, "Study on the thermal-magnetic coupling characteristics of integrated eddy current retarder," in *Proc. World Congr. Exhib.*, no. 5, Apr. 2016, pp. 1884–2021.

[13] J. Tian, D. Li, K. Ning, and L. Ye, "Research on heat dissipation optimization of a novel liquid-cooling eddy current brake," *IEEE Trans. Energy Convers.*, early access, Jul. 7, 2020, doi: 10.1109/TEC.2020.3007752.

[14] T. Lubin and A. Rezzoug, "Steady-state and transient performance of axial-field eddy-current coupling," *IEEE Trans. Ind. Electron.*, vol. 62, no. 4, pp. 2287–2296, Apr. 2015.

[15] K.-H. Shin, H.-I. Park, H.-W. Cho, and J.-Y. Cho, "Semi-three-dimensional analytical torque calculation and experimental testing of an eddy current brake with permanent magnets," *IEEE Trans. Appl. Supercond.*, vol. 28, no. 3, Jan. 2018, Art no. 5203205.

[16] J. Wang and J. Zhu, "A simple method for performance prediction of permanent magnet eddy current couplings using a new magnetic equivalent circuit model," *IEEE Trans. Ind. Electron.*, vol. 65, no. 3, pp. 2487–2495, Mar. 2018.

[17] W. Kemmetmüller, D. Faustner, and A. Kugi, "Modeling of a permanent magnet synchronous machine with internal magnets using magnetic equivalent circuits," *IEEE Trans. Magn.*, vol. 50, no. 6, Jun. 2014, Art. no. 8101314.

XIANGLI LI was born in Jining, China, in 1996. He received the B.S. degree from Jining University, Jining, in 2018. He is currently pursuing the M.S. degree with the Faculty of Material Manufacturing, Beijing University of Technology.

He is currently involved in the design, analysis, and optimization of eddy-current brake.

LEZHI YE received the B.S. degree from the North China University of Technology, Beijing, China, in 2005, and the M.S. and Ph.D. degrees from the Beijing University of Technology, Beijing, in 2008 and 2012, respectively. He is currently a Teacher with the Faculty of Material Manufacturing, Beijing University of Technology. His research interests include vehicle retarder and electronic packaging technology.

MINGFEI LI was born in Henan, China, in 1996. He received the B.S. degree from the Henan University of Technology, Zhengzhou, China, in 2018. He is currently pursuing the M.S. degree with the Faculty of Material Manufacturing, Beijing University of Technology.

He is currently involved in the analysis of eddy-current brake.

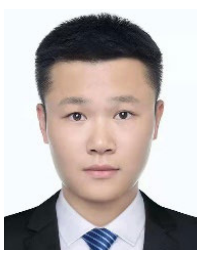

QIANG LV was born in Henan, China, in 1995. He received the B.S. degree from Henan Agricultural University, Zhengzhou, China, in 2018. He is currently pursuing the M.S. degree with the Faculty of Material Manufacturing, Beijing University of Technology.

He is currently involved in the design of eddy-current brake.